Configuration-interaction Monte Carlo method and its application to the trapped unitary Fermi gas

Abhishek Mukherjee[1,2] and Y. Alhassid[1]

[1]*Center for Theoretical Physics, Sloane Physics Laboratory, Yale University, New Haven, Connecticut 06520, USA*

[2]*European Centre for Theoretical Studies in Nuclear Physics and Related Areas, Villa Tambosi, I-38123 Villazzano, Trento, Italy*

(Received 17 April 2013; published 18 November 2013)

We develop a quantum Monte Carlo method to estimate the ground-state energy of a fermionic many-particle system in the configuration-interaction shell model approach. The fermionic sign problem is circumvented by using a guiding wave function in Fock space. The method provides an upper bound on the ground-state energy whose tightness depends on the choice of the guiding wave function. We argue that the antisymmetric geminal product class of wave functions is a good choice for guiding wave functions. We demonstrate our method for the trapped two-species fermionic cold atom system in the unitary regime of infinite scattering length using the particle-number projected Hartree-Fock-Bogoliubov wave function as the guiding wave function. We estimate the ground-state energy and energy-staggering pairing gap as a function of the number of particles. We compare our results with exact numerical diagonalization results and with previous fixed-node coordinate-space Monte Carlo calculations.

DOI: 10.1103/PhysRevA.88.053622 PACS number(s): 67.85.−d, 02.70.Ss, 21.60.Cs, 21.60.Ka

I. INTRODUCTION

The configuration-interaction (CI) shell-model approach is widely used in nuclear, atomic, and molecular physics. It accounts for both shell effects and correlations in finite-size many-particle systems (see, e.g., Refs. [1,2]). The CI many-particle model space for an N-fermion system is a truncated space spanned by N-particle Slater determinants constructed from a given finite single-particle basis. An effective CI Hamiltonian is defined in this truncated space.

When the many-particle model space is sufficiently small, the CI Hamiltonian can be diagonalized by conventional methods. However, the combinatorial increase of the dimensionality of the many-particle space versus the size $\mathcal{N}_s$ of the single-particle basis and/or the number of particles N prohibits direct diagonalization for large $\mathcal{N}_s$ and/or N. This difficulty can be overcome in part by using quantum Monte Carlo methods for which the computational effort scales much more gently with the size of the single-particle model space. An example is the auxiliary-field Monte Carlo (AFMC) method. The AFMC approach has been applied within the CI framework to nuclei [3–6] (where the method is known as the shell-model Monte Carlo method), and more recently to the cold atomic condensate in a harmonic trap [7].

Other quantum Monte Carlo methods include coordinate-space ("**r**-space") Monte Carlo methods, e.g., diffusion Monte Carlo (DMC) and Green's-function Monte Carlo (GFMC) [8]. These methods filter out the ground state with the help of an appropriately defined projection operator or a propagator. A GFMC method that works on a discrete lattice in coordinate space (known as lattice GFMC) was also developed [9–11].

Here we introduce a configuration-interaction Monte Carlo (CIMC) method that provides an upper bound on the ground-state energy of a fermionic system in the CI framework. Our method builds on techniques developed in the lattice GFMC method. A discrete configuration space is defined by the occupation numbers of the single-particle states and an initial configuration-space wave function is propagated in imaginary time. The sign problem is circumvented by introducing a propagator that depends on a guiding wave function and keeps the wave function positive semidefinite. The method yields an upper bound on the ground-state energy whose accuracy (as an estimate of the ground-state energy) depends on the choice of the guiding wave function. We argue that the use of antisymmetric geminal product (AGP) wave functions [12] as guiding wave functions offers a good compromise between accuracy and computational efficiency.

We demonstrate the CIMC method by applying it to the trapped two-species fermionic cold atom system in the unitary limit of infinite scattering length. We use the particle-number projected Hartree-Fock-Bogoliubov (HFB) wave function (a member of the AGP class) as the parameter-free guiding wave function. Cold atomic gases have recently attracted much interest both experimentally and theoretically [13,14]. The interaction strength in these systems can be controlled by tuning the scattering length near a Fano-Feshbach resonance. Since these systems depend on a small number of parameters, they are useful for testing many-body methods of strongly interacting systems. The unitary limit is particularly challenging since, in the absence of a small parameter, it is not amenable to perturbative treatments.

II. THE CONFIGURATION-INTERACTION MONTE CARLO (CIMC) METHOD

Our method consists of two main components: (i) projecting on the ground-state wave function through a random walk in configuration space, and (ii) circumventing the fermionic sign problem with the help of a guiding wave function.

We assume a general CI Hamiltonian which includes only two-body interactions

$$H = \sum_{a\in\mathcal{S}} \varepsilon_a a_a^\dagger a_a + \frac{1}{2}\sum_{abcd\in\mathcal{S}} V_{abcd} a_a^\dagger a_b^\dagger a_c a_d, \tag{1}$$

where $a_a^\dagger$ creates a particle in the single-particle state labeled by a. The set $\mathcal{S}$ of single-particle states is assumed to be finite of size $\mathcal{N}_s$.

We define an operator $\mathcal{P}$ by

$$\mathcal{P} = 1 - \Delta\tau(H - E_T), \tag{2}$$

where E_T is an energy shift (to be discussed later). This operator can be used to propagate in imaginary time a wave function in the many-particle space from τ to $\tau + \Delta\tau$ by

$$|\Psi_{\tau+\Delta\tau}\rangle = \mathcal{P}|\Psi_\tau\rangle. \tag{3}$$

The ground-state wave function $|\Psi_{\rm gs}\rangle$ can be projected out by the repeated application of $\mathcal{P}$ on an initial wave function Ψ_0 that has a nonzero overlap with $\Psi_{\rm gs}$, i.e.,

$$|\Psi_{\rm gs}\rangle = \lim_{\tau\to\infty} |\Psi_\tau\rangle, \tag{4}$$

provided the eigenvalues of $\mathcal{P}$ are between -1 and 1. The latter condition implies that the time step $\Delta\tau$ satisfies $\Delta\tau < 2/(E_{\rm max} - E_T)$, where $E_{\rm max}$ is the maximal eigenvalue of H. Equation (4) is exact and there is no error that depends on the size of the time step.

The method works in the N-particle Hilbert space that is spanned by the set of all N-particle Slater determinants constructed from the single-particle orbitals $a \in \mathcal{S}$. We will denote these Slater determinants or "configurations" by $|\mathbf{n}\rangle$, where $\mathbf{n} \equiv \{n_a\}$ and $n_a = 0,1$ is the occupation number of orbital a. The one-step propagation (3) can be written in the configuration representation as

$$\Psi_{\tau+\Delta\tau}(\mathbf{m}) = \sum_{\mathbf{n}} \langle \mathbf{m}|\mathcal{P}|\mathbf{n}\rangle \Psi_\tau(\mathbf{n}), \tag{5}$$

where $\Psi_\tau(\mathbf{n}) \equiv \langle \mathbf{n}|\Psi_\tau\rangle$ is the wave function representation in configuration space. We rewrite the configuration-space matrix elements of $\mathcal{P}$ in the form

$$\langle \mathbf{m}|\mathcal{P}|\mathbf{n}\rangle = g(\mathbf{n})p(\mathbf{m},\mathbf{n}), \tag{6}$$

where

$$g(\mathbf{n}) = \sum_{\mathbf{m}} \langle \mathbf{m}|\mathcal{P}|\mathbf{n}\rangle, \tag{7}$$

and

$$p(\mathbf{m},\mathbf{n}) = \frac{\langle \mathbf{m}|\mathcal{P}|\mathbf{n}\rangle}{g(\mathbf{n})}. \tag{8}$$

We first consider the case when the matrix elements of $\mathcal{P}$ are all non-negative, i.e., $\langle \mathbf{m}|\mathcal{P}|\mathbf{n}\rangle \geqslant 0$ for all $\mathbf{m}$ and $\mathbf{n}$. Then $0 \leqslant p(\mathbf{m},\mathbf{n}) \leqslant 1$ with $\sum_{\mathbf{m}} p(\mathbf{m},\mathbf{n}) = 1$ and $g(\mathbf{n}) \geqslant 0$, and we can interpret $p(\mathbf{m},\mathbf{n})$ for fixed $\mathbf{n}$ as a probability and $g(\mathbf{n})$ as a weight. This enables us to carry out the propagation of Ψ_τ in (5) stochastically as follows. Assuming at a given time τ the wave function Ψ_τ is non-negative in configuration space, i.e., $\Psi_\tau(\mathbf{n}) \geqslant 0$ for all $\mathbf{n}$, the wave function Ψ_τ can be represented as an ensemble of configurations $\mathbf{n}$. According to (5) and the non-negativity of the matrix elements of $\mathcal{P}$, the wave function remains non-negative at $\tau + \Delta\tau$, i.e., $\Psi_{\tau+\Delta\tau}(\mathbf{m}) \geqslant 0$ for all $\mathbf{m}$. For each configuration $\mathbf{n}$, a new configuration $\mathbf{m}$ is chosen with probability $p(\mathbf{m},\mathbf{n})$ and replicated with weight $g(\mathbf{n})$. The resulting ensemble of configurations $\{\mathbf{m}\}$ samples the wave function $|\Psi_{\tau+\Delta\tau}\rangle$ at the next imaginary-time step $\tau + \Delta\tau$. We note that in CIMC, the diffusion in configuration space is determined by the interaction part of the Hamiltonian, while in coordinate-space Monte Carlo methods it is the kinetic part which governs the diffusion.

After a sufficiently large number of time steps, the contribution from excited states to $|\Psi_\tau\rangle$ becomes negligible. Ensembles generated at subsequent time steps are considered as representatives of $|\Psi_{\rm gs}\rangle$ and a decorrelated subset of these ensembles is used to calculate observables.

As mentioned above, the propagation with $\mathcal{P}$ filters out the ground state when the time step satisfies $\Delta\tau < 2/(E_{\rm max} - E_T)$. This upper bound for $\Delta\tau$ becomes smaller with increasing N and/or $\mathcal{N}_s$ since $E_{\rm max}$ gets larger. Consequently, the number of time steps required for decorrelation and for projecting the ground state increases. This makes the simple algorithm described above inefficient for large $\mathcal{N}_s$ and/or N.

We overcome this latter difficulty by using an algorithm proposed in Ref. [15]. We start by choosing a finite imaginary time step $\delta\tau$ (which is different from $\Delta\tau$). Assuming the configuration $\mathbf{n}$ is a member of the ensemble at time τ, we describe the choice of the corresponding configuration and its replication weight at time $\tau + \delta\tau$. We define a propagation time $\delta\tau_p$ that is initially set to $\delta\tau$ and a weight g that is initially set to 1. We then sample a time $\delta\tau_d$ for an off-diagonal move from the (un-normalized) probability distribution $e^{-\pi_d\delta\tau_d}$, where $\pi_d = \sum_{\mathbf{m}\neq\mathbf{n}} \langle \mathbf{m}|H - E_T|\mathbf{n}\rangle$. If $\delta\tau_d \geqslant \delta\tau_p$, then $\mathbf{n}$ remains unchanged in the next time step and is replicated with the weight $g = e^{-\delta\tau_p \sum_{\mathbf{m}} \langle \mathbf{m}|H-E_T|\mathbf{n}\rangle}$. Otherwise, a new configuration $\mathbf{n}'$ is chosen with probability $\langle \mathbf{n}'|H - E_T|\mathbf{n}\rangle/\pi_d$ ($\mathbf{n}' \neq \mathbf{n}$), and the weight factor is multiplied by $e^{-\delta\tau_d \sum_{\mathbf{m}} \langle \mathbf{m}|H-E_T|\mathbf{n}\rangle}$. This process is repeated with the replacements $\mathbf{n} \to \mathbf{n}'$ and $\delta\tau_p \to \delta\tau_p - \delta\tau_d$ until we have $\delta\tau_d \geqslant \delta\tau_p$. This algorithm generates the probability distribution $p(\mathbf{m},\mathbf{n})$ and weight $g(\mathbf{n})$ that correspond to the propagator $e^{-\delta\tau(H-E_T)} = \lim_{\Delta\tau\to 0} \mathcal{P}^{\delta\tau/\Delta\tau}$ without any time step errors due to the finiteness of $\delta\tau$ [11].

The above algorithm breaks down if $p(\mathbf{m},\mathbf{n}) < 0$, i.e., if $\langle \mathbf{m}|H|\mathbf{n}\rangle > 0$ for a given pair of configurations $\mathbf{m} \neq \mathbf{n}$. For a general CI Hamiltonian, this might be the case and is the manifestation of the Monte Carlo sign problem for our method.[1]

In continuum $\mathbf{r}$-space Monte Carlo methods the sign problem is circumvented with the help of a fixed-node approximation, which can be used to obtain an upper bound on the ground-state energy. However, in the CI approach the Hilbert space is labeled by discrete quantum numbers. It was shown in lattice GFMC that a fixed-node-like approximation can be introduced to obtain an upper bound on the ground-state energy also for discrete Hilbert spaces. In the following we show how this can be formulated for a CI Hamiltonian.

We choose a guiding wave function Φ_G and define for any configurations $\mathbf{n}$ and $\mathbf{m}$ with $\Phi_G(\mathbf{n}) \neq 0$ the quantity

$$\mathfrak{s}(\mathbf{m},\mathbf{n}) \equiv \Phi_G(\mathbf{m})\langle \mathbf{m}|H|\mathbf{n}\rangle/\Phi_G(\mathbf{n}). \tag{9}$$

We then introduce a family of Hamiltonians $\mathcal{H}_\gamma$ defined over configurations $\mathbf{n}$ with $\Phi_G(\mathbf{n}) \neq 0$ such that the off-diagonal

[1] An important exception is the pairing Hamiltonian, for which a diffusion Monte Carlo algorithm free of a sign problem can be formulated within the CI framework using the occupations of time-reversed pairs [16,17].

matrix elements are given by [9–11]

$$\langle \mathbf{m}|\mathcal{H}_\gamma|\mathbf{n}\rangle = \begin{cases} -\gamma\langle \mathbf{m}|H|\mathbf{n}\rangle & \mathfrak{s}(\mathbf{m},\mathbf{n}) > 0, \\ \langle \mathbf{m}|H|\mathbf{n}\rangle & \text{otherwise}, \end{cases} \tag{10}$$

while the diagonal matrix elements are

$$\langle \mathbf{n}|\mathcal{H}_\gamma|\mathbf{n}\rangle = \langle \mathbf{n}|H|\mathbf{n}\rangle + (1+\gamma) \sum_{\substack{\mathbf{m}\neq\mathbf{n} \\ \mathfrak{s}(\mathbf{m},\mathbf{n})>0}} \mathfrak{s}(\mathbf{m},\mathbf{n}). \tag{11}$$

We note that $\mathcal{H}_{\gamma=-1} = H$. We define a γ-dependent propagator $\mathcal{P}_\gamma$ for configurations $\mathbf{n}$ with $\Phi_G(\mathbf{n}) \neq 0$ by

$$\langle \mathbf{m}|\mathcal{P}_\gamma|\mathbf{n}\rangle = 1 - \Delta\tau\,\Phi_G(\mathbf{m})\langle \mathbf{m}|\mathcal{H}_\gamma - E_T|\mathbf{n}\rangle/\Phi_G(\mathbf{n}). \tag{12}$$

Using Eqs. (10) and (11) in Eq. (12), the diagonal matrix elements of $\mathcal{P}_\gamma$ are given by

$$\langle \mathbf{n}|\mathcal{P}_\gamma|\mathbf{n}\rangle = 1 - \Delta\tau \left(\langle \mathbf{n}|H|\mathbf{n}\rangle - E_T + (1+\gamma) \sum_{\substack{\mathbf{m}\neq\mathbf{n} \\ \mathfrak{s}(\mathbf{m},\mathbf{n})>0}} \mathfrak{s}(\mathbf{m},\mathbf{n}) \right) \tag{13}$$

and are non-negative for a sufficiently small $\Delta\tau$. The off-diagonal matrix elements are

$$\langle \mathbf{m}|\mathcal{P}_\gamma|\mathbf{n}\rangle = \begin{cases} \gamma\Delta\tau\,\mathfrak{s}(\mathbf{m},\mathbf{n}) & \mathfrak{s}(\mathbf{m},\mathbf{n}) > 0, \\ -\Delta\tau\,\mathfrak{s}(\mathbf{m},\mathbf{n}) & \text{otherwise}. \end{cases} \tag{14}$$

Thus, for $\gamma \geqslant 0$ (and sufficiently small $\Delta\tau$), the propagator $\mathcal{P}_\gamma$ satisfies $\langle \mathbf{m}|\mathcal{P}_\gamma|\mathbf{n}\rangle \geqslant 0$ for any $\mathbf{m}$ and $\mathbf{n}$, and is therefore free of the sign problem. The stochastic projection algorithm outlined above can then be generalized with the replacement of $\langle \mathbf{m}|H|\mathbf{n}\rangle$ by $\Phi_G(\mathbf{m})\langle \mathbf{m}|\mathcal{H}_\gamma|\mathbf{n}\rangle/\Phi_G(\mathbf{n})$. This stochastic projection filters out the wave function $\Phi_G(\mathbf{n})\Psi_\gamma(\mathbf{n})$, where $\Psi_\gamma(\mathbf{n})$ is the ground-state wave function of $\mathcal{H}_\gamma$.

The ground-state energy $\mathcal{E}_\gamma$ of H_γ [in the nonsingular space $\Phi_G(\mathbf{n}) \neq 0$] is an upper bound for the ground-state energy E_0 of the original Hamiltonian H for $\gamma \geqslant 0$. This result is derived in Refs. [10,11] for the case when Φ_G is nonzero for all configurations in the Hilbert space. In the following we derive this result for the case where $\Phi_G(\mathbf{n})$ may vanish for certain configurations (this is typically the situation for CI guiding wave functions). In this case the propagator $\mathcal{P}_\gamma$ is nonsingular only in the subspace of configurations $\mathbf{n}$ spanned by $\Phi_G(\mathbf{n}) \neq 0$. The Hamiltonian $\mathcal{H}_\gamma$ is also nonsingular in this subspace. The energy $\mathcal{E}_\gamma$ is an upper bound for the ground-state energy of H when restricted to this nonsingular subspace [10,11]. This latter energy is an upper bound on E_0 (which is the ground-state energy of H in the full Hilbert space). Thus, $\mathcal{E}_\gamma$ is an upper bound on E_0.

It is seen from Eq. (12) that as long as the initial ensemble includes only those configurations for which $\Phi_G(\mathbf{n}) \neq 0$, the Monte Carlo projection does not reach configurations $\mathbf{m}$ for which $\Phi_G(\mathbf{m}) = 0$. Thus, the Monte Carlo projection correctly finds the ground-state energy in the space where $\mathcal{P}_\gamma$ is nonsingular and provides an upper bound on E_0.

One can verify using Eqs. (10) and (11) that $\langle \Phi_G|\mathcal{H}_\gamma|\Phi_G\rangle = \langle \Phi_G|H|\Phi_G\rangle$. Since $\mathcal{E}_\gamma$ is the ground-state energy of $\mathcal{H}_\gamma$, $\mathcal{E}_\gamma \leqslant \langle \Phi_G|\mathcal{H}_\gamma|\Phi_G\rangle = \langle \Phi_G|H|\Phi_G\rangle$, i.e., the upper bounds on E_0 given by $\mathcal{E}_\gamma$ are tighter than the variational upper bound with Φ_G.

The energies $\mathcal{E}_\gamma$ are estimated using the "mixed" estimate for the Hamiltonian $\mathcal{H}_\gamma$,

$$\mathcal{E}_\gamma = \frac{\sum_{\mathbf{n}} \mathcal{E}^L(\mathbf{n})\Phi_G(\mathbf{n})\Psi_\gamma(\mathbf{n})}{\sum_{\mathbf{n}} \Phi_G(\mathbf{n})\Psi_\gamma(\mathbf{n})} \approx \frac{1}{N_E}\sum_i \mathcal{E}^L(\mathbf{n}_i), \tag{15}$$

where N_E is the size of the ensemble $\{\mathbf{n}_i\}$ representing $\Phi_G(\mathbf{n})\Psi_\gamma(\mathbf{n})$ and $\mathcal{E}^L(\mathbf{n}) = \langle \Phi_G|\mathcal{H}_\gamma|\mathbf{n}\rangle/\Phi_G(\mathbf{n}) = \langle \Phi_G|H|\mathbf{n}\rangle/\Phi_G(\mathbf{n})$ is the so-called local estimate of the energy.

The energy shift E_T is used to control the size of the configuration population. It is adjusted infrequently during the evolution to keep the population of configurations roughly constant and provides an independent estimate (the "growth" estimate) of the ground-state energy of $\mathcal{H}_\gamma$. However, its statistical error is typically much larger than that of the mixed estimate in Eq. (15).

The finite time step $\delta\tau$ is kept fixed throughout the entire calculation. In principle, its value is arbitrary since the method is free from time step errors. However, if $\delta\tau$ is too large, then the configuration population undergoes large fluctuations between consecutive time steps. On the other hand, if $\delta\tau$ is too small, then the number of time steps required to decorrelate the energy becomes very large. As a compromise we choose an intermediate value for $\delta\tau$.

A linear extrapolation of $\mathcal{E}_\gamma$ from any two values of $\gamma \geqslant 0$ to $\gamma = -1$ also provides an upper bound on E_0 that is tighter than the individual $\mathcal{E}_\gamma$ [18]. This follows from

$$H = \mathcal{H}_{-1} = \frac{1}{\gamma_2 - \gamma_1}\left[(1+\gamma_2)\mathcal{H}_{\gamma_1} - (1+\gamma_1)\mathcal{H}_{\gamma_2}\right] \tag{16}$$

implying that

$$\begin{aligned}\langle \Psi_{\gamma_1}|H|\Psi_{\gamma_1}\rangle = \frac{1}{\gamma_2-\gamma_1}[&(1+\gamma_2)\langle \Psi_{\gamma_1}|\mathcal{H}_{\gamma_1}|\Psi_{\gamma_1}\rangle \\ &- (1+\gamma_1)\langle \Psi_{\gamma_1}|\mathcal{H}_{\gamma_2}|\Psi_{\gamma_1}\rangle].\end{aligned} \tag{17}$$

Using the standard Rayleigh-Ritz variational principle we have $E_0 = \langle \Psi_{\rm GS}|H|\Psi_{\rm GS}\rangle \leqslant \langle \Psi_{\gamma_1}|H|\Psi_{\gamma_1}\rangle$ and $\mathcal{E}_{\gamma_2} = \langle \Psi_{\gamma_2}|\mathcal{H}_{\gamma_2}|\Psi_{\gamma_2}\rangle \leqslant \langle \Psi_{\gamma_1}|\mathcal{H}_{\gamma_2}|\Psi_{\gamma_1}\rangle$. Together with

$\langle\Psi_{\gamma_1}|\mathcal{H}_{\gamma_1}|\Psi_{\gamma_1}\rangle = \mathcal{E}_{\gamma_1}$ we obtain

$$E_0 \leqslant \frac{1}{\gamma_2-\gamma_1}[(1+\gamma_2)\mathcal{E}_{\gamma_1} - (1+\gamma_1)\mathcal{E}_{\gamma_2}]. \tag{18}$$

The right-hand side in the above inequality is precisely the linear extrapolation from any two values γ_1 and γ_2 to $\gamma = -1$.

We found that the best compromise between the tightness of the upper bound and the size of the statistical error in the extrapolation is obtained for $\gamma_1 = 0$ and $\gamma_2 = 1$. This choice gives $E_{\mathrm{CIMC}} = 2\mathcal{E}_{\gamma=0} - \mathcal{E}_{\gamma=1}$ as our best upper bound for the ground-state energy E_0.

The tightness of the energy upper bound is determined to a large extent by the quality of the guiding wave function. If the guiding wave function is the exact ground-state wave function (i.e., $\Phi_G = \Psi_{\mathrm{gs}}$), then $\mathcal{E}_\gamma = E_0$ for all γ. Furthermore, for Φ_G close to Ψ_{gs} the difference $\mathcal{E}_\gamma - E_0$ is second order in $\Phi_G - \Psi_{\mathrm{gs}}$ [10]. Thus, the accuracy of the CIMC method can be improved by systematically improving the quality of the guiding wave function.

Ideally, Φ_G should encode all our *a priori* knowledge about the ground-state wave function. However, for the CIMC method to be practical, we should be able to calculate Φ_G efficiently and accurately. As we discussed above, the configuration space in which the stochastic projection is carried out is determined by the condition $\Phi_G \neq 0$. It is preferable for this space to be sufficiently large so as to include the dominant correlations.

In coordinate-space Monte Carlo methods, optimized Slater-Jastrow or BCS-Jastrow wave functions are examples of highly accurate yet efficient guiding wave functions. For a CI Hamiltonian, a good choice is provided by the AGP class of wave functions [12]. The most general AGP wave function for an even N-particle system is given by

$$|\Phi_{\mathrm{AGP}}\rangle = \left(\sum_{ab}\phi_{ab}a_a^\dagger a_b^\dagger\right)^{N/2}|0\rangle, \tag{19}$$

where $|0\rangle$ is the particle vacuum. The coefficients ϕ_{ab} are the "geminals" which encode information about the correlations in the system. The AGP wave functions incorporate important two-body correlations yet they are described by a single Pfaffian, i.e., $\Phi_{\mathrm{AGP}}(\mathbf{n})$ is the Pfaffian of an $N \times N$ matrix [19]. This latter property ensures their efficient numerical evaluation. More recently, AGP wave functions have also been used extensively in coordinate-space quantum Monte Carlo calculations (see, e.g., in Ref. [20]). We emphasize that while our estimate always provides an upper bound for the ground-state energy, the tightness of this upper bound depends on the choice of the guiding wave function and cannot be predicted *a priori*.

III. APPLICATION TO THE TRAPPED UNITARY FERMI GAS

To demonstrate the CIMC method, we consider the two-species (labeled by spin up and spin down) fermionic cold atom system, in which atoms with opposite spins interact via a short-range interaction, modeled by a contact interaction $\delta(\mathbf{r}-\mathbf{r}')$. The CI many-body Hamiltonian of this system in an isotropic harmonic trap is given by

$$H = \sum_{i\in\mathcal{S}}\varepsilon_i(a_{i\uparrow}^\dagger a_{i\downarrow} + a_{i\downarrow}^\dagger a_{i\downarrow}) + g\hbar\omega\left(\frac{\hbar}{m\omega}\right)^{3/2} \times \sum_{ijkl\in\mathcal{S}}\langle ij|\delta(\mathbf{r}-\mathbf{r}')|kl\rangle a_{i\uparrow}^\dagger a_{j\downarrow}^\dagger a_{l\downarrow}a_{k\uparrow}, \tag{20}$$

where ω, m, and ε_i are, respectively, the frequency of the trap, the particle mass, and the single-particle energies in an isotropic harmonic trap. The label i denotes a single-particle state in orbital space and $\uparrow,\downarrow$ denote spin-up and spin-down particles.

The dimensionless coupling strength g for finite $\mathcal{N}_s$ is determined by the condition that the two-particle ground-state energy in the laboratory frame reproduces the exact energy [7]. In the unitary limit of infinite scattering length the exact two-particle ground-state energy is $2\hbar\omega$ [21]. We note that the renormalization of the contact interaction in a finite model space is a nontrivial problem and there exist more rigorous treatments of the effective interaction [22–24].

We choose the single-particle model space $\mathcal{S}$ to include all single-particle orbitals within $\mathcal{N}_{\mathrm{max}}$ harmonic oscillator shells, i.e., with energy $\varepsilon_i \leqslant (\mathcal{N}_{\mathrm{max}} + \frac{3}{2})\hbar\omega$. A model space with $\mathcal{N}_{\mathrm{max}} = 9$ has $\mathcal{N}_s = 440$ single-particle states. The respective many-particle space for $N = 20$ particles has dimension $\sim 10^{35}$.

For this system it is reasonable to assume that the dominant correlations are in the pairing and particle-hole channels. A wave function that includes these correlations is described by the HFB approximation. The HFB wave function does not conserve particle number, thus it is necessary to project it on a fixed number of particles. We only consider here even-N spin-balanced systems and odd-N systems with one unbalanced spin-up particle. The particle-number projected Hartree-Fock-Bogoliubov (PHFB) wave function (projection after variation) belongs to the AGP class of wave functions. For the even-N ($N = 2n$) system it is given by

$$|\Phi_{\mathrm{PHFB}}^e\rangle = \left(\sum_{ijk}\frac{v_k}{u_k}D_{ik}D_{jk}a_{i\uparrow}^\dagger a_{j\downarrow}^\dagger\right)^n|0\rangle, \tag{21}$$

where the matrix D describes the transformation to the canonical basis, and u_k, v_k are the coefficients of the Bogoliubov transformation in the canonical basis [25].

For the odd-N ($N = 2n+1$) system, the wave function belongs to the generalized AGP class of wave functions and is given by

$$|\Phi_{\mathrm{PHFB}}^o\rangle = \left(\sum_i D_{ib}a_{i\uparrow}^\dagger\right)\left(\sum_{\substack{ij\\k\neq b}}\frac{v_k}{u_k}D_{ik}D_{jk}a_{i\uparrow}^\dagger a_{j\downarrow}^\dagger\right)^n|0\rangle, \tag{22}$$

where b is the "blocked" spin-up orbital in the canonical basis. The configuration-space representations of $\Phi_{\mathrm{PHFB}}^e(\mathbf{n})$ and $\Phi_{\mathrm{PHFB}}^o(\mathbf{n})$ are determinants of $n \times n$ and $(n+1)\times(n+1)$ matrices, respectively.

The particle-number projected Bardeen-Cooper-Schrieffer (PBCS) and Hartree-Fock (HF) wave functions have similar forms. In PBCS the D matrix is the identity, while in HF $v_k/u_k = \theta(k_F - |k|)$ with k_F being the highest occupied

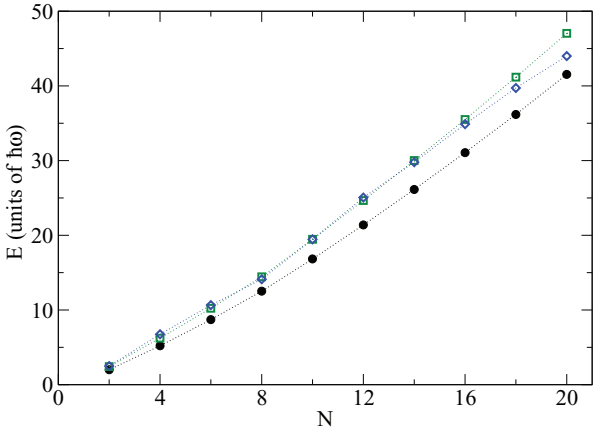

FIG. 1. (Color online) The CIMC ground-state energy estimates vs particle number N for $\mathcal{N}_{\max} = 6$ at unitarity using the renormalized Hamiltonian described in the text for different choices of the guiding wave function: PHFB (solid circles), PBCS (open squares), and HF (open diamonds). The statistical errors are smaller than the size of the symbols in all cases.

orbital in the canonical basis. Generally, the quantities D_{ij}, u_k, and v_k have to be recalculated self-consistently depending on the particular wave function we use, e.g., the values of u_k, v_k in PHFB are different from their values in PBCS.

The PBCS wave function includes correlations in the pairing channel only, while the HF wave function includes correlations in the particle-hole channel only. We expect the PHFB wave function, which includes correlations in both channels to be superior to either of those. This expectation is confirmed in Fig. 1 where we compare the CIMC ground-state energy estimates at the unitary limit for different choices of the guiding wave function: HF, PBCS, and PHFB in a truncated model space of $\mathcal{N}_{\max} = 6$ oscillator shells. The energy estimates provided by the PHFB guiding wave function are much lower than those of the HF and PBCS wave functions for all values of the particle number N.

Next we investigate the quality of the PHFB wave function as a guiding wave function. To this end, we compare in Table I the CIMC energies using the PHFB as the guiding wave function with the exact results for smaller values of $\mathcal{N}_{\max}$ and N for which exact numerical diagonalization is possible [24,26]. We find that for an even (odd) number of particles the CIMC energies are within 1% (2–3%) of the exact results.

For larger systems, exact numerical diagonalization is not possible. However, **r**-space fixed-node DMC results are available [27–29]. In Fig. 2 we compare the CIMC ground-state energies using $\mathcal{N}_{\max} = 9$ (solid circles) with fixed-node DMC calculations for $N \leqslant 20$. The CIMC ground-state energies using $\mathcal{N}_{\max} = 9$ oscillator shells are 0.5–3% higher than those obtained in Ref. [27]. The ground-state energy estimates from Ref. [28] (open diamonds) are typically slightly higher than those in Ref. [27] (open squares) but with larger statistical error. The latest state-of-the-art **r**-space fixed-node DMC energies reported in Ref. [29] (open inverted triangles) further improve the results of Ref. [27]. At $\mathcal{N}_{\max} = 9$ the differences between the CIMC energies for successive values of $\mathcal{N}_{\max}$ become smaller than their statistical errors. We have not carried out any $\mathcal{N}_{\max} \to \infty$ extrapolations in this work.

TABLE I. Comparison of the CIMC ground-state energies vs the exact ground-state energies for a CI model space of $\mathcal{N}_{\max} = 3$ and $\mathcal{N}_{\max} = 8$, and for several values of the particle number N. For the CIMC energies, the numbers in parentheses denote the statistical error in the last significant digit. The $\mathcal{N}_{\max} = 3$ energies were obtained using the OXBASH code [26], while the $\mathcal{N}_{\max} = 8$ energies were obtained using a serial version of the diagonalization code developed in Ref. [24].

		Ground-state energy [units of $\hbar\omega$]	
$\mathcal{N}_{\max}$	N	CIMC	Exact
3	6	8.639(7)	8.601
	7	11.176(4)	11.021
	8	12.292(7)	12.179
8	2	2.000(6)	2.000
	3	4.391(4)	4.279
	4	5.208(9)	5.138

In Fig. 3 we compare the energy-staggering pairing gaps Δ calculated in the CIMC method with the pairing gaps obtained from the **r**-space GFMC calculations of Refs. [27,28]. We have also included the pairing gaps obtained from the density functional theory calculations of Ref. [30]. The energy-staggering pairing gap for an odd-N system is defined by

$$\Delta = E_0(N) - \tfrac{1}{2}[E_0(N-1) + E_0(N+1)], \qquad (23)$$

where $E_0(N)$ is the ground-state energy for N particles. Our results seem to be consistent with the results of Refs. [27,30], although the CIMC statistical errors are much smaller than the statistical errors of the fixed-node DMC calculations. The nonsmooth behavior at $N = 7$ is probably due to the shell closure at $N = 8$.

For the results shown here we used $\sim 2 \times 10^5$ independent configurations for the calculation of each energy. In most cases, the initial ensemble consisted of the noninteracting ground state. We also verified in a few test cases that the final result does not depend on the choice of the initial

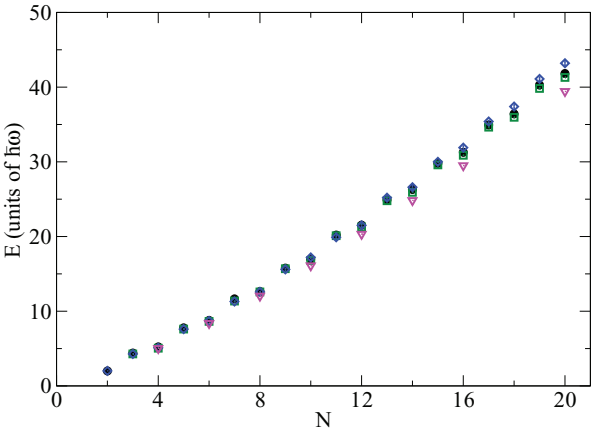

FIG. 2. (Color online) The ground-state energy at unitarity for $N \leqslant 20$ particles. The CIMC results for $\mathcal{N}_{\max} = 9$ (solid circles) are compared with fixed-node DMC results of Ref. [27] (open squares), Ref. [28] (open diamonds), and Ref. [29] (open inverted triangles). The statistical errors are smaller than the size of the symbols.

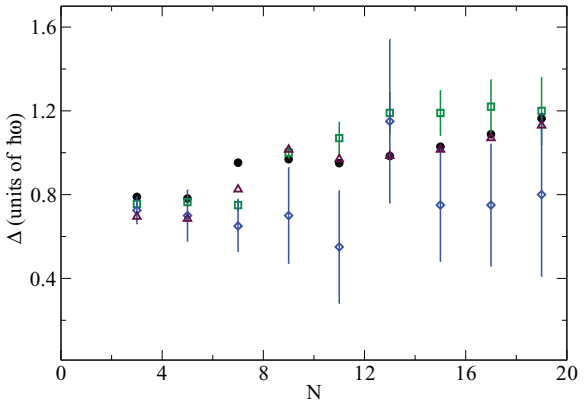

FIG. 3. (Color online) Energy-staggering pairing gap vs number of atoms N. Our CIMC results for $\mathcal{N}_{\max} = 9$ (solid circles) are compared with similar gaps calculated in Ref. [27] (open squares), Ref. [28] (open diamonds), and Ref. [30] (open triangles). The vertical bars describe the statistical errors. The CIMC errors are smaller than the size of the symbols.

ensemble. The calculations for $\mathcal{N}_{\max} \leqslant 4$ were carried out on a single processor and took up to a few hours. For $\mathcal{N}_{\max} > 4$ the calculations were performed on a cluster. The largest calculation with $\mathcal{N}_{\max} = 9$ and $N = 20$ took about 900 cpu hours. We choose $\delta\tau \sim 0.1$ for these calculations. With this choice the number of time steps required to project the ground state was $\sim$100 and the number of decorrelation time steps was $\lesssim$5. We did not find any significant dependence of the optimal $\delta\tau$, projection time, or decorrelation time on $\mathcal{N}_s$ or N.

The nominal scaling of the computational effort for the CIMC method with an AGP guiding wave function is $\sim N^2(\mathcal{N}_s - N)^2 \times N^3 \sim N^5(\mathcal{N}_s - N)^2$ where the factor $N^2(\mathcal{N}_s - N)^2$ originates in the maximal number of possible nonzero matrix elements in Eq. (6) for a given $\mathbf{n}$, while the factor N^3 is the computational effort required to calculate a Pfaffian or a determinant of an $N \times N$ matrix. The prefactor in this scaling can vary significantly depending on the type of interaction. For example, in the system described above with interactions between up and down spins only, there are only $(N/2)^2\{(\mathcal{N}_s - N)/2\}^2$ nonzero terms in Eq. (6) and we only have to calculate the determinant of an $N/2 \times N/2$ matrix. Thus, the computational effort in this case is about two orders of magnitude smaller than in the most general case.

IV. DISCUSSION AND CONCLUSION

It is interesting to compare our method with the constrained-path Monte Carlo [31] and the full CI quantum Monte Carlo [32] methods. Both of these methods perform a stochastic projection of the ground-state wave function in Fock space similar to our method. In the constrained-path Monte Carlo method, the Hamiltonian is "linearized" with the help of the Hubbard-Stratanovich transformation and the random walk is carried out in the continuous space of the auxiliary fields. The sign problem is circumvented with the help of a guiding wave function. However, the mixed energy estimate in this method is not an upper bound on the true ground-state energy. In the full CI quantum Monte Carlo method, the random walk is carried out in the discrete configuration space as in our method. No guiding wave function is used in this method, and the sign problem is mitigated using a configuration-annihilation algorithm. However, the computational effort in this method scales with the size of the many-particle space (i.e., it is exponential in $\mathcal{N}_s$ and N), although it is a fraction of the computational effort involved in direct diagonalization methods.

In conclusion, we have introduced a CIMC algorithm that provides an upper bound for the ground-state energy of a finite fermionic system in the CI approach. The main advantage of this method as compared with coordinate-space DMC is that it can be also used to treat nonlocal interactions for which the CI approach is more natural. We argue that the AGP class of wave functions provides a good choice for guiding wave functions. We demonstrate the CIMC method for the trapped cold atom Fermi gas condensate at unitarity using the PHFB wave function as a guiding wave function. For a small number of particles and sufficiently small number of single-particle orbitals, we find that the CIMC ground-state energies are within a few percent of the exact results. Our CIMC results for number of particles $N \leqslant 20$ are consistent with previous coordinate-space DMC calculations.

We emphasize that the CIMC method described here is quite general and can be applied to other fermionic systems such as cold atoms in a deformed trap and finite nuclei. It can also be used to calculate properties other than the ground-state energy such as the average occupation numbers. It will be interesting to determine whether the energy upper bounds can be improved by using other choices for the geminals in the AGP wave function, or by using other classes of wave functions.

ACKNOWLEDGMENTS

We thank C. N. Gilbreth for useful discussions and for his help in providing some of the exact results in Table I, and S. Gandolfi for providing their fixed-node DMC results shown in Fig. 2. This work was supported in part by Department of Energy Grant No. DE-FG-0291-ER-40608. Computational cycles were provided by the facilities of the Yale University Faculty of Arts and Sciences High Performance Computing Center.

[1] I. Talmi, *Simple Models of Complex Nuclei: The Shell Model and Interacting Boson Model* (Harwood Academic, Switzerland, 1993).

[2] A. Szabo and N. S. Ostlund, *Modern Quantum Chemistry: Introduction to Advanced Electronic Structure Theory* (Dover, New York, 1996), Chap. 4.

[3] G. H. Lang, C. W. Johnson, S. E. Koonin, and W. E. Ormand, Phys. Rev. C **48**, 1518 (1993).

[4] Y. Alhassid, D. J. Dean, S. E. Koonin, G. Lang, and W. E. Ormand, Phys. Rev. Lett. **72**, 613 (1994).

[5] S. E. Koonin, D. J. Dean, and K. Langanke, Phys. Rep. **278**, 1 (1997).

[6] Y. Alhassid, Int. J. Mod. Phys. B **15**, 1447 (2001).
[7] C. N. Gilbreth and Y. Alhassid, arXiv:1210.4131.
[8] *Quantum Monte Carlo Methods in Physics and Chemistry*, edited by M. P. Nightingale and C. J. Umrigar (Kluwer, Amsterdam, 1999).
[9] H. J. M. van Bemmel, D. F. B. ten Haaf, W. van Saarloos, J. M. J. van Leeuwen, and G. An, Phys. Rev. Lett. **72**, 2442 (1994).
[10] D. F. B. ten Haaf, H. J. M. van Bemmel, J. M. J. van Leeuwen, W. van Saarloos, and D. M. Ceperley, Phys. Rev. B **51**, 13039 (1995).
[11] S. Sorella and L. Capriotti, Phys. Rev. B **61**, 2599 (2000).
[12] A. J. Coleman and V. I. Yukalov, in *Reduced Density Matrices* (Springer-Verlag, New York, 2000), Chap. 4.
[13] I. Bloch, J. Dalibard, and W. Zwerger, Rev. Mod. Phys. **80**, 885 (2008).
[14] S. Giorgini, L. P. Pitaevskii, and S. Stringari, Rev. Mod. Phys. **80**, 1215 (2008).
[15] N. Trivedi and D. M. Ceperley, Phys. Rev. B **41**, 4552 (1990).
[16] N. Cerf and O. Martin, Phys. Rev. C **47**, 2610 (1993).
[17] A. Mukherjee, Y. Alhassid, and G. F. Bertsch, Phys. Rev. C **83**, 014319 (2011).
[18] M. Beccaria, Phys. Rev. B **64**, 073107 (2001).
[19] A. J. Coleman, J. Mol. Struct.: THEOCHEM **527**, 75 (2000); M. Bajdich, L. Mitas, G. Drobný, L. K. Wagner, and K. E. Schmidt, Phys. Rev. Lett. **96**, 130201 (2006); M. Bajdich, L. Mitas, L. K. Wagner, and K. E. Schmidt, Phys. Rev. B **77**, 115112 (2008).
[20] J. Kolorenč and L. Mitas, Rep. Prog. Phys. **74**, 026502 (2011).
[21] T. Busch, B. G. Englert, K. Rzaewski, and M. Wilkens, Found. Phys. **28**, 549 (1998); S. Jonsell, Few-Body Syst. **31**, 255 (2002).
[22] I. Stetcu, B. R. Barrett, U. van Kolck, and J. P. Vary, Phys. Rev. A **76**, 063613 (2007).
[23] Y. Alhassid, G. F. Bertsch, and L. Fang, Phys. Rev. Lett. **100**, 230401 (2008).
[24] C. N. Gilbreth and Y. Alhassid, Phys. Rev. A **85**, 033621 (2012).
[25] P. Ring and P. Schuck, *The Nuclear Many-Body Problem* (Springer, Berlin, 1980).
[26] B. A. Brown, A. Etchegoyen, and W. D. M. Rae, MSU-NSCL Report No. 524, 1988.
[27] D. Blume, J. von Stecher, and C. H. Greene, Phys. Rev. Lett. **99**, 233201 (2007).
[28] S. Y. Chang and G. F. Bertsch, Phys. Rev. A **76**, 021603(R) (2007).
[29] M. M. Forbes, S. Gandolfi, and A. Gezerlis, Phys. Rev. Lett. **106**, 235303 (2011); Phys. Rev. A **86**, 053603 (2012); J. Carlson, S. Gandolfi, and A. Gezerlis, Prog. Theor. Exp. Phys. 01A209 (2012).
[30] A. Bulgac, Phys. Rev. A **76**, 040502(R) (2007).
[31] S. Zhang, J. Carlson, and J. E. Gubernatis, Phys. Rev. Lett. **74**, 3652 (1995); Phys. Rev. B **55**, 7464 (1997).
[32] G. H. Booth, A. J. W. Thom, and A. Alavi, J. Chem. Phys. **131**, 054106 (2009); D. Cleland, G. H. Booth, and A. Alavi, *ibid.* **132**, 041103 (2010); G. H. Booth, A. Grüneis, G. Kresse, and A. Alavi, Nature (London) **493**, 365 (2013).